A multidisciplinary characterization of a tailings pond in the Linares-La Carolina mining district, Spain

J. Martínez [a,*], M.C. Hidalgo [b], J. Rey [b], J. Garrido [c], C. Kohfahl [d], J. Benavente [e], D. Rojas [b]

[a] Department of Mechanical and Mining Engineering, Higher Polytechnic School of Linares, University of Jaen, 23700 Linares, Spain
[b] Department of Geology, Higher Polytechnic School of Linares, University of Jaén, 23700 Linares, Spain
[c] Department of Civil Engineering, Higher Technical School of Civil Engineering, University of Granada, 18071 Granada, Spain
[d] IGME, Sevilla, Subdelegación de Gobierno Pza, de España, Torre Norte, 41013, Sevilla, Spain
[e] Water Research Institute, University of Granada, c/ Ramón y Cajal, no. 4, 18071 Granada, Spain

ABSTRACT

Geochemical and geophysical techniques have been applied to investigate the potential environmental impact of the abandoned La Aquisgrana mine tailings, one of the most important sulfide-bearing tailings ponds of the Linares-La Carolina mining district (Spain). The geometry of the pile has been defined through geological field work and electrical resistivity imaging (ERI) surveys. The ERI profiles revealed the position of the bedrock surface below the tailings central area (more than 40 m in thickness) and helped in placing drill core sampling for geochemical analysis and a piezometer installation. In the 21 extracted samples, the total content of Pb, Zn, Cu, Fe, Mn, Sr, Rb and As were determined, with significant values being found for Pb and Zn ($>$2000 mg kg^{-1}), Mn ($>$700 mg kg^{-1}) and As ($>$170 mg kg^{-1}). Although AMD has not been identified, water samples from the saturated zone of the tailings are characterized by elevated dissolved sulfate (2495 mg L^{-1}), Fe (20 mg L^{-1}), Mn (16 mg L^{-1}) and Zn (7 mg L^{-1}) contents, with an E.C. value of 3.3 mS cm^{-1} and pH from 5.6 to 6.9, suggesting a process of metal mobilization. Physical and chemical data obtained from drill core and groundwater samples were combined with the electrical resistivity profile of the tailings to characterize areas with higher metal concentrations. A central low resistivity area ($<$30 Ω.m) was identified in the vadose zone of the pile, correlated with higher Fe, Zn, Pb, As, and sulfide concentrations, and with a significant increase in silt and clay content. The lowest resistivity values ($<$5 Ω.m) were measured in the saturated zone of the tailings, related with the highest metal(oid) contents in both solid phase and water. A lower resistivity area close to the fractured zone of the bedrock suggests a preferential flow path for subsurface water infiltration. The generated geophysical–geochemical model has allowed to depict areas of the tailings characterized by high metallic and water contents that present the greater risk for contamination.

© 2015 Elsevier B.V. All rights reserved.

1. Introduction

The Linares-La Carolina metallic mining district (southern Spain, Jaén province, Fig. 1) is characterized by vein deposits that are primarily composed of lead and copper sulfides (Castelló and Orviz 1976). These mineralizations have been the subject of intense historical exploitation, but were abandoned during the late 20th century. The mineralogical industry was developed in parallel, with the creation of numerous gravimetric and flotation plants. Until the mid-1950s, only gravimetric techniques were used to determine mineral concentrations. The waste products were typically deposited in heaps located near the mining facilities, sometimes

possessing high mineral grades due to the technical limitations of these processes (Gutiérrez-Guzmán 1999; Contreras and Dueñas 2010).

During the second half of the 20th century, a flotation process was introduced to separate and concentrate metal-bearing mineralin the Linares-La Carolina mining district. The flotation technique resulted in significant advances in the mineral processing industry, allowing nearly 100% of all metal content to be recovered via mining, a percentage that was virtually unthinkable using traditional gravimetric methods. In fact, ancient mine wastes with higher metal grade contents were rewashed using flotation to obtain their metallic contents. The final waste products were deposited in tailings ponds, often with no prior land preparation. This created considerable environmental risks. At least 32 large tailings impoundments have been identified in this mining district (Gutiérrez-Guzmán 1999; Martínez 2002; Contreras and Dueñas 2010). Significant attention is
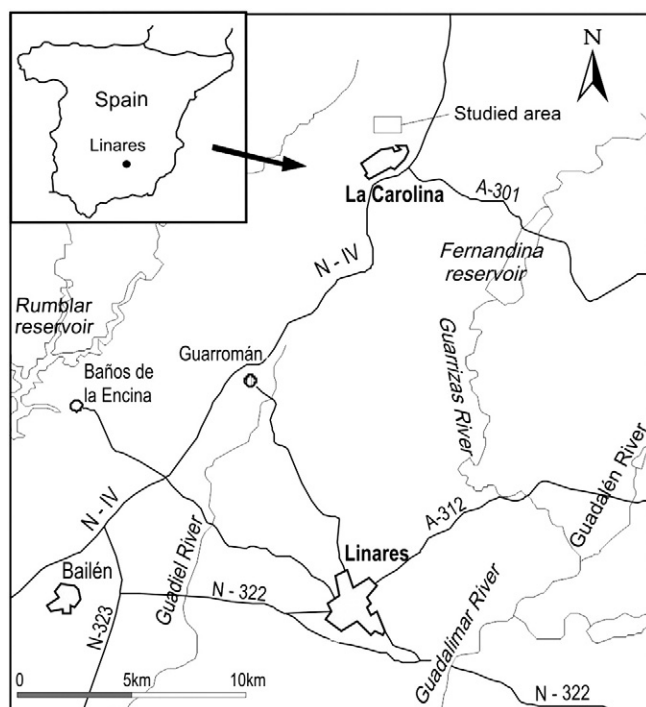
Fig. 1. Location of the study region.

currently given to the management of these potentially hazardous materials.

Thus, the main objectives of this study are to:

a) Identify the deposited residue levels that may present a contamination risk through the combined use of geophysical and geochemical techniques.
b) Characterize the tailings and provide data for planning of remediation actions.

The La Aquisgrana mine tailings, one of the most important tailings impoundments in the district, were selected, based on its size (with a total volume of around one million m^3) and its location. It is situated in an agricultural area with olive groves and close to the La Campana River floodplain, suggesting potential soil and water environmental risks. These studies have a special interest for the control of tailings from other mining regions, where the exploitation, mineral recovery and metallurgy processes represent major heavy metal sources (Davis 1983; Li and Thornton 1993, 2001; Chopin and Alloway 2007; Chae Jung 2008; Bundschuh et al. 2012; Gómez-Ros et al. 2013; Domínguez et al. 2016).

2. Description of the study area

The La Aquisgrana mine tailings pond is one of the largest (200 × 180 × 35 m) and most representative of the La Carolina mining district. It is situated in the La Carolina municipality, 2 km to the north of the town, close to the remains of the La Aquisgrana abandoned washery (Fig. 2, Fig. 3A).

The La Aquisgrana mine was operated from 1899 to 1983. The exploited ore consists of hydrothermal Pb–Ag veins and Cu–Fe sulfides, which is hosted by metamorphic rocks, such as phyllites with sporadic quartzite layers (Lillo 1992). Specifically, the mineral paragenesis consists of:

a) Pb–Ag sulfantimonites, with galena being the main ore, along with cerussite and anglesite. Silver sulfantimonites occur as minor ore minerals, and ankerite is the predominant gangue.

b) Cu–Fe sulfides, of which chalcopyrite, pyrite and marcasite are the main ores, sphalerite and galena are the minor ores, and quartz, calcite and chlorite are the main gangue minerals.

In 1973, a flotation plant was constructed to rewash the former gravimetric heaps located in the vicinity of the mineral exploitation (Gutiérrez-Guzmán 2007). The flotation flow-sheet consisted of finely grinding the graded mixtures, with waste sizes of <16 mm. The pulp was taken to a closed-cycle Denver-type classifier to separate particles with Tyler mesh sizes of less than 48 (0.297 mm). Larger sizes were returned to the mill. Upon reaching the optimal size, pulp that contained 42% solids was transferred to the flotation process. Denver dual-cell, 80 × 80 cm sub-ventilation equipment was used to perform roughing, cleaning and scavenging processes. The most commonly used collectors were sodium and potassium oxalate. Long-chain aliphatic alcohols were typically used as foaming agents along with pine oil. Sodium cyanide was used as a depressor, which forms zinc cyanide with $ZnSO_4$. This depresses iron sulfide, arsenopyrite and sphalerite, and also has the beneficial effect of serving as a desilter. $CaCO_3$ and $Ca(OH)_2$ were used as regulating agents to attain a basic bath with a pH between 8 and 10, which is ideal for galena flotation. Finally, a fine concentration was obtained with lead concentrations approaching 75% (Contreras and Dueñas 2010).

The tailings were dumped on Palaeozoic phyllite substrate. The tailings impoundment was built from a small dike of spoiled materials. It is situated in a valley, with the tailings occupying the riverbeds of two tributary creeks of the La Campana River, which flows by the foot of the impoundment. The runoff from the creeks is channeled by a drainage pipe at the bottom of the tailings, which discharges into the La Campana River. The top of the tailings is positioned on a slight southwestward facing slope, which collects water during the rainy season. In addition, the slope features substantial surface erosion, cracks and local landslides. In addition, bank erosion occurs on the lower sections of the slope during large flood events, undermining the overall structure.

De la Torre et al. (2010) studied the mineralogy of tailings from the La Carolina district. Two samples were taken from the first 30–50 cm of La Aquisgrana tailings and studied using X-ray diffraction (XRD) and a scanning electron microscope (SEM). The results indicate that the tailings are primarily comprised of quartz and phyllosilicates, which are very abundant. Feldspars, calcite, ankerite, cerussite and galena were also identified as trace minerals. Precipitated salts from the surface of the tailings were also analyzed. Gypsum was the predominant mineral phase, but Fe sulfate with As and Zn was also present.

3. Methodology

3.1. Geophysical surveys

A geophysical survey was conducted using Electrical Resistivity Imaging (ERI). This technique has been previously used for tailings analyzes (Martínez-Pagán et al. 2009, 2011; Gómez-Ortiz et al. 2010; Martín-Crespo et al. 2010; Placencia-Gómez et al. 2010; Martínez et al. 2012, 2014; Martín-Crespo et al. 2012, 2015; Zarroca et al. 2015).

This is a non-destructive geoelectrical method that analyzes underground materials based on their electrical behavior, differentiating based on electrical resistivity (Telford et al. 1990; Store et al. 2000). The method consists of implanting electrodes over a profile, with a pre-determined separation based on the degree of sensitivity and depth to be analyzed. A higher sensitivity is obtained when the electrodes are placed closer, but wider spaced electrodes allow for scanning at greater depths (Loke and Barker 1996; Loke and Dahlin 2002; Dahlin and Zhou 2004). Technically, an electrical-resistivity imaging survey can be conducted using different electrode arrays (e.g., dipole–dipole, pole–pole, pole–dipole, Wenner, Schlumberger or Wenner–Schlumberger)
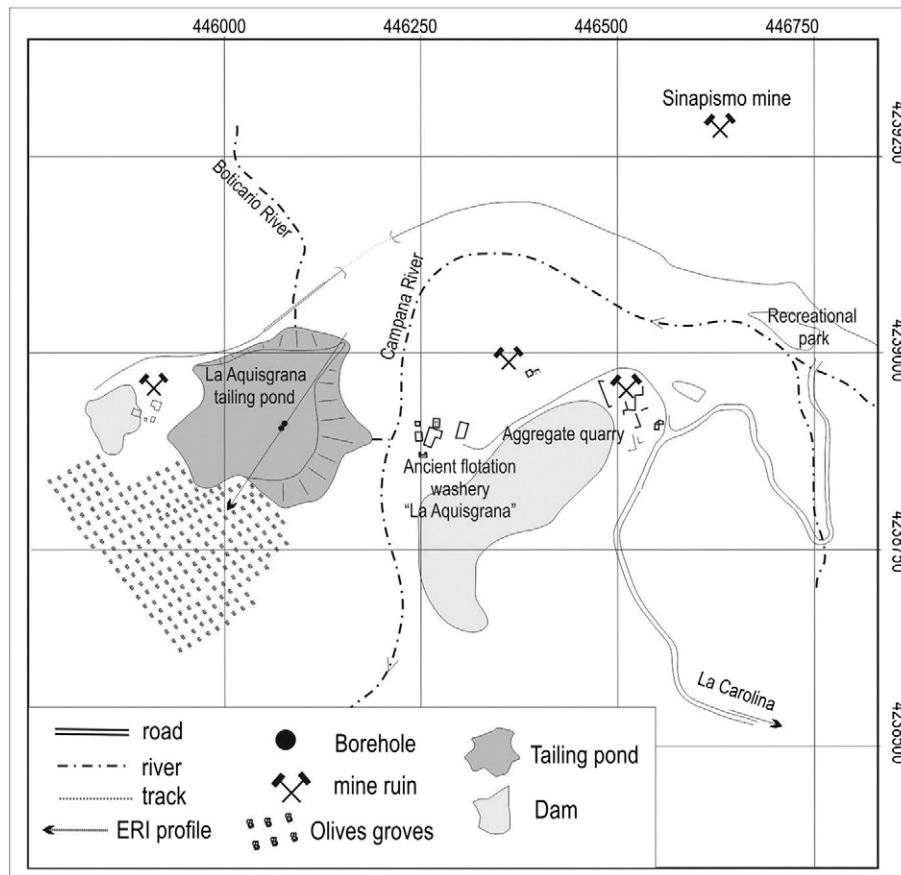
Fig. 2. Location of the La Aquisgrana tailings impoundment, showing the position of the ERI profile and boreholes.

that are spread across the surface. Creating an optimal array is a matter of significant debate in the literature (e.g., Zhou and Dahlin 2003; Dahlin and Zhou; Drahor 2006). The "best" array choice for a field survey depends on the type of structure to be mapped, the sensitivity of the resistivity meter and the background noise level (Loke and Dahlin 2002).

The Wenner–Schlumberger array is a hybrid between the Wenner and Schlumberger arrays. This array is moderately sensitive to both horizontal and vertical structures. In areas where both types of geological structures are expected, this array represents a good compromise between the Wenner and the dipole–dipole arrays. The median depth of investigation for this array is approximately 10% larger than that for the Wenner array for the same distance between the outer electrodes. The signal strength for this array is smaller than that for the Wenner array, but it is higher than the dipole–dipole array (Sasaki, 1992; Loke and Dahlin 2002). This array has been successfully used in similar studies (Gómez-Ortiz et al. 2010; Martín-Crespo et al. 2010, 2012, 2015; Martínez et al. 2012, 2014) because of the high resistivity contrast between the tailings beds and their infill.

The piece of electrical tomography equipment used in this study was the Deutsche Montan Technologie (DMT) RESECS model. This multielectrode device has an integrated computer that can manage up to 960 electrodes.

ERI profile interpretation was conducted based on the real resistivities obtained during field work, which were treated with specific RES2DINV resistivity software (Griffiths and Barker 1993). This calculation program utilizes the least squares method with forced smoothing, which is modified with the Quasi-Newton optimization technique. The reversal method creates an underground model based on rectangular prisms and determines the resistivity values for each prism, minimizing the difference between the apparent and the calculated resistivity values (Loke and Barker 1996, Loke and Dahlin 2002). In our study, a total of 96 electrodes were installed at a spacing of 3 m. This ensured identification of the tailing pond details and geometry, as well as its relationship with the substrate at an adequate resolution.

Thus, ERI profiling was conducted on a cross-section of the La Aquisgrana tailings in a NE–SW direction (Fig. 2) using the Wenner–Schlumberger method. The total profile length was 290 m, reaching a depth of 42 m. In total, 2012 apparent resistivity measurements were taken.

3.2. Mechanical surveys

During the beginning of autumn 2012, three boreholes were drilled (Figs. 2 and 3B) in the La Aquisgrana tailings in close proximity. They were situated on the ERI line after conducting and interpreting the geoelectrical profile, based on a position with the maximum tailing infill thickness that contacted the phyllitic bedrock (Fig. 4). One borehole was drilled using a triple core barrel. It had a diameter of 86 mm and was used to produce stratigraphic logs and samples. The other boreholes were drilled with a simple core barrel and had 113 mm diameters. They were used for installing various sensors.

The first borehole was drilled to 40.3 m and was continuously sampled (Fig. 3C). The phyllites were found at 39.8 m below the tailings. Sediment analyses were performed on 21 drill core samples (Fig. 3D) from the depths of 1, 3, 4, 5, 6, 7, 8.5, 10, 13, 15.5, 17, 21.5, 23, 26.5, 29.5, 31, 34, 35.5, 38.5, 39 and 39.4 m. A piezometric casing was installed to control the tailings saturated zone. The second borehole was drilled 2 m to the NE of the first hole, reaching the phyllites at 37.5 m. Sensors were installed at 3 different depths (35.5, 23 and 13 m). They measured the oxygen content. A third borehole was drilled to 6.5 m and four sensors were installed at shallower depths (1, 3, 5 and 6 m deep).
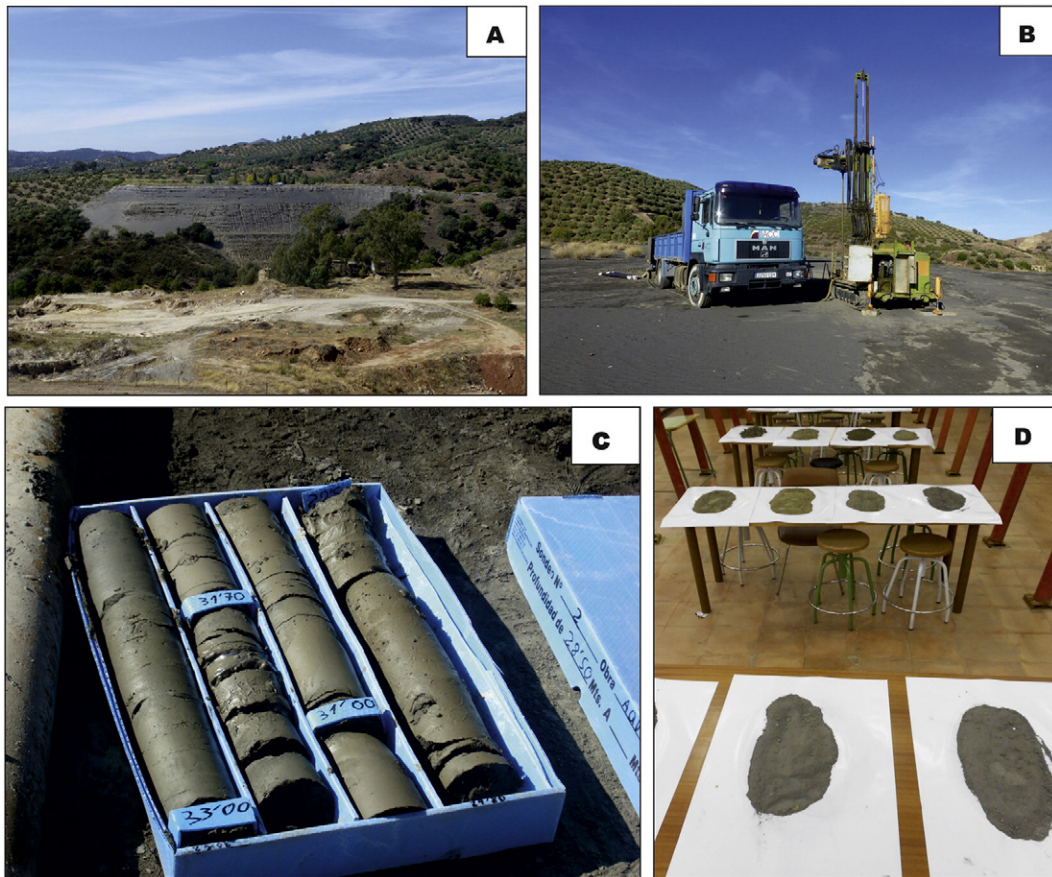
Fig. 3. General view of the La Aquisgrana tailings (a), where the ancient washery ruins can be seen in the foreground. Drilling operations (b). A box filled with drill cores (c). Drill core samples in the laboratory (d).

Fig. 4. Interpretation of the Electrical Resistivity Imaging profile: apparent resistivity sections (a); real resistivity sections (b). The boundary between the tailings and the substratum is highlighted with a white dotted line. The position of the profile is shown in Fig. 2.

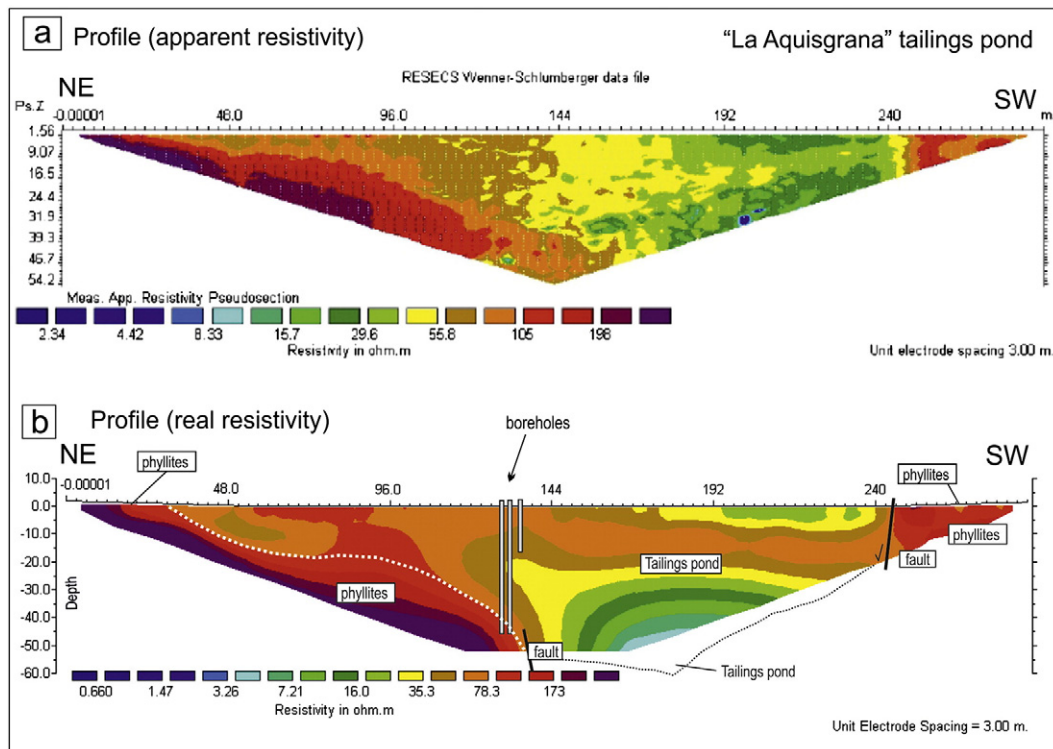The sensors were placed inside the borehole, which was filled with the same material as the tailings. The oxygen content was measured using PreSens fiber optic probes (model PSt3) and a Presens Fibox 3 LCD model data logger.

3.3. Geochemical data

Geochemical characterizations were conducted for the 21 drill core samples obtained from the borehole, including total metal content (Pb, Zn, Cu, As, Mn, Sr, Rb and Fe), pH, $CaCO_3$, total sulfide, humidity and sand-silt-clay fraction analyses (Tables 1 and 2). Humidity was measured by gravimetric method and expressed as wt.% of water. Sieving method was used to separate the sand fraction, and the clay and silt fractions were determined by sedimentation. Metal content was determined based on the X-ray fluorescence of the sample (NITON XLt 792 Analyzer) after it was ground in an agate mortar. The pH measurements were conducted in a 1:2.5 suspension of the sample and distilled water using an XS Instruments model 510 pH-meter. The calcium carbonate percentage was determined via the Bernard calcimeter method and the total sulfide content was analyzed according to the UNE-EN 1744-1 method.

Water samples were collected from the piezometer at 37 m of depth to analyze major and trace elements. Seven sampling campaigns were performed in different seasons from November 2012 to January 2014. The water was filtered in the field using a 0.45-μm filter, and the samples were preserved via the addition of nitric acid at a pH less than 2.5. Electrical conductivity (E.C.) and temperature were measured in the field using a WTW LF92 meter, while pH, Eh and O_2 were measured with a Hach Lange HQ20 meter.

3.4. Statistical analysis

Univariate and multivariate analysis techniques were used to identify relationships, compare and group data, and facilitate its interpretation (Reimann and Filzmoser 2000; Reimann and Garret 2005; Yuan et al. 2014).

Table 2
pH, $CaCO_3$, total sulfide content, humidity and percentage values of clay, silt and sand fractions for the drill core samples.

	Sample depth (m)	pH	CaCO₃ (%)	S²⁻ (%)	Humidity (%)	Clay (%)	Silt (%)	Sand (%)
Tailings pond	1	7.7	2.2	0.33	12.3	15	15	70
	3	8.0	4.4	0.40	10.13	30	32.5	37.5
	4	8.0	6.6	0.40	12.2	15	15	70
	5	8.3	8.1	0.39	14.1	20	15	65
	6	8.2	8.6	0.37	11.4	25	25	50
	7	8.3	8.2	0.48	9.9	15	15	70
	8.5	8.1	4.9	0.37	8.4	20	20	60
	10.2	8.0	3.1	0.23	18.6	20	20	60
	13	6.8	0.9	0.50	30.6	20	25	55
	15.5	8.0	2.4	0.03	8.6	20	25	55
	17	7.7	2.9	0.36	11.7	15	17.5	67.5
	21.5	7.6	4.3	0.26	25.6	37.5	32.5	30
	23	7.6	3.4	0.55	10.7	30	50	20
	26.3	7.6	3.2	0.46	20.0	25	30	45
	29.4	7.8	3.3	0.60	24.5	25	40	35
	31	7.5	3.1	0.28	34.2	40	50	10
	34	7,5	1.7	0.43	18.6	20	25	55
	35.5	7.2	1.7	0.49	24.7	15	25	60
	38.5	7.0	1.4	0.35	29.4	35	35	30
	39.3	6.7	2.1		25.4	40	45	15
Phyllites	39.4	6.5	0.7	0.21	20.9	17.5	25	57.5

Cluster analyses allow for the separation of individuals into natural groups based on proximity criteria, with the discrepancies between individuals and groups being minimized while the distance separating each group is maximized. Ward's clustering criteria and the Euclidean distance measure were used to measure divergence. Agglomerative hierarchical clustering was used, separating the two most similar groups of each step from both the groups and the conjunctions of individual specimens, until one group was attained (Huang et al. 1994; Kalogeropulos et al. 1994; Ruiz et al. 1998; Facchinelli et al. 2001; Gallego et al. 2002; Yongming et al. 2006; Guo-Li et al. 2013). Statistical analyses were carried out using the SPSS 19.0 program for Windows and MINITAB Release 10 for Windows.

Table 1
Metal(oid) concentrations in drill core samples. The guidelines for the maximal allowable concentrations of Pb, Zn, Cu and As (mg kg⁻¹) established by law are also included: (a) allowable levels and (b) compulsory treatments in agricultural soil.

		CONTENTS (mg kg⁻¹)							wt.%
	Sample depth (m)	Pb	Zn	Cu	As	Mn	Sr	Rb	Fe
TAILINGS POND	1	3153	1442	41	76	728	56	122	2.5
	3	3195	1977	531	69	722	40	110	2.1
	4	664	1528	35	45	780	29	115	2.0
	5	916	1747	33	76	900	29	108	1.8
	6	1033	1812	39	78	888	28	114	1.8
	7	1084	1778	49	70	987	29	114	1.9
	8.5	1534	1476	33	50	798	29	116	1.9
	10.2	751	1675	35	129	657	25	99	1.7
	13	1412	3540	29	544	676	25	106	2.5
	15.5	1838	2071	37	253	805	26	108	2.2
	17	1504	2273	39	158	655	30	94	1.6
	21.5	2424	1521	36	150	790	28	120	2.0
	23	2591	1821	32	194	751	28	118	2.1
	26.3	2579	2156	36	154	647	27	111	2.0
	29.4	1471	1833	37	135	713	25	102	1.8
	31	3075	2127	41	179	875	27	131	2.3
	34	976	2280	30	270	640	25	102	1.9
	35.5	1655	1956	29	218	537	25	96	1.9
	38.5	6237	2616	60	333	492	35	121	3.0
	39.3	8065	5186	53	423	534	37	141	3.5
Phyllites	39.4	485	692	40	43	138	77	101	1.8
	Average content	2308	2141	63	180	729	30	112	2.1
	Maximun allowed (a)	100–200	200–300	50–100	<20				
	Compulsory treatment (b)	350–500	600–1000	300–500	>50				

4. Results

4.1. Geophysical surveys

Fig. 4 presents the profiles of the apparent and real resistivity values obtained for the La Aquisgrana tailings. The materials found in the tailings exhibited real resistivity values ranging from 10 to 100 Ω.m (Fig. 4b). The Palaeozoic substrate possessed higher values (>100 Ω.m) than the tailings, so it was generally easy to detect contact between the two units.

High resistivity values were observed in the NE section of the profile, ranging from 150 to 250 Ω.m. They correspond to Palaeozoic substrate phyllites, which outcrop in this area. However, the phyllites are mylonitized by the presence of a large fracture zone in the SW section, presenting much lower resistivity values. The presence of this fracture can be deduced both via outcrops and geophysical profiles (Fig. 4).

Low resistivity values were detected in the shallow tailings of the SW section, which cover the Palaeozoic phyllites. This was interpreted as a preferred infiltration area, where high moisture levels cause decreased resistivity. A 15 m interspersed level can be identified deeper
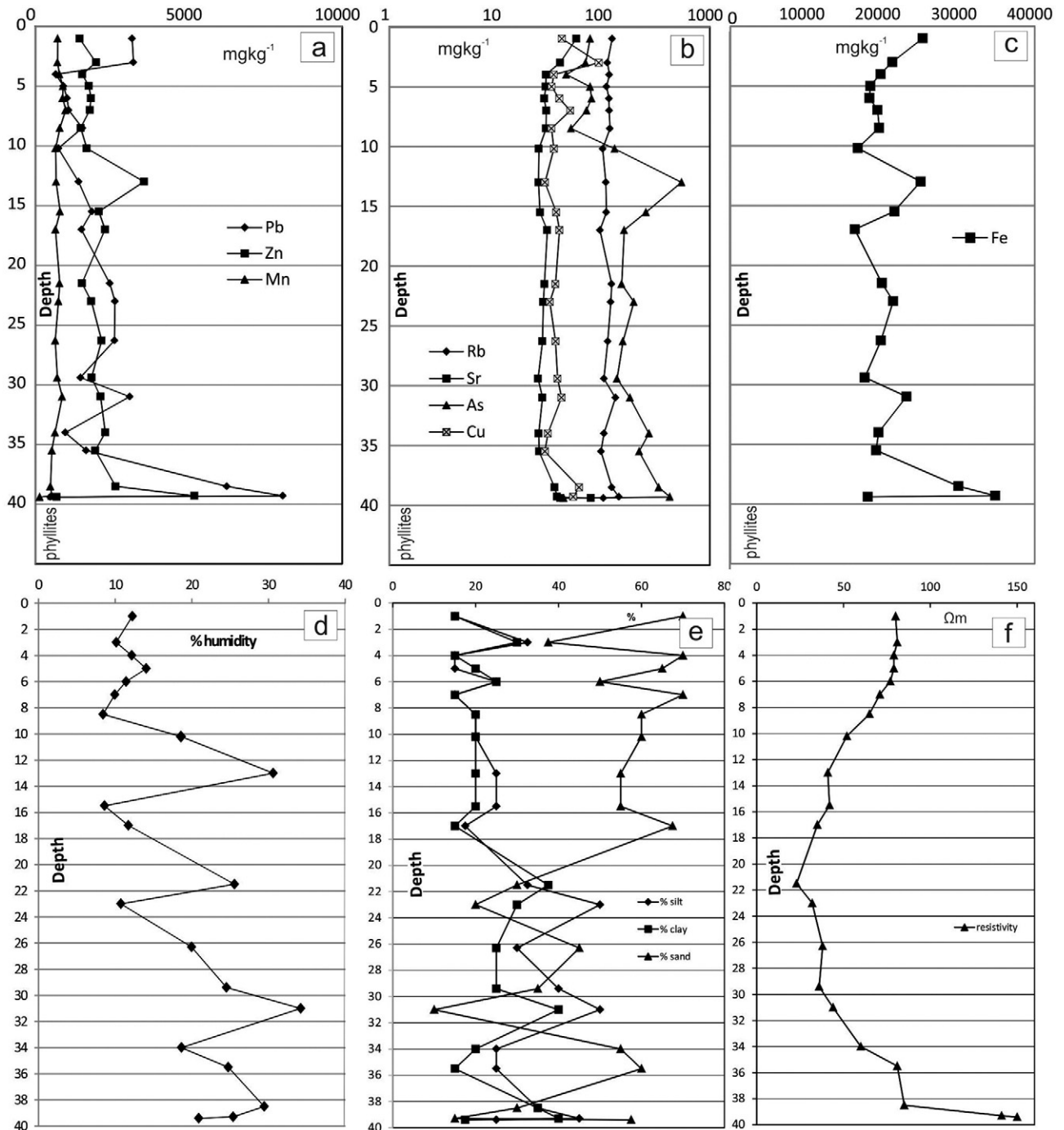

Fig. 5. Variation with depth of selected physical–chemical parameters: Pb, Zn and Mn (a); Rb, Sr, As and Cu (b); Fe (c); humidity percentages (d); clay–silt–sand percentages (d); real resistivity values along the borehole (e).

into the profile, with resistivity values ranging from 50 to 100 Ω.m. It can be identified as fine permeable sands and silt. The base of the pond, with an average thickness of 25 m, exhibited a real resistivity decrease from 50 to 3 Ω.m., which can be attributed to an increase in the silt and clay fraction of the tailings and a higher humidity. The lowest values (5–10 Ω.m) are associated with the existence of a saturated zone in the core of the tailings.

In addition, this area corresponds to an old ravine, as inferred from the field surveys. The geophysical profile was not deep enough to reach the contact between the tailings and the basement in the central tailings zone, which can be expected at more than 50 m deep. Unfortunately, the topography of the area does not allow for longer ERI lines, which could potentially increase the penetration depth of the resistivity profile.

4.2. Mechanical surveys

According to the particle size distribution analysis of the 21 drill core samples, the tailings are mostly sandy, with varying amounts of silt and clay. The moisture ranged from 8.4 to 14.1% in the first 9 m of the borehole and from 18 to 30% in the last 15 m of the borehole, respectively (Table 2 and Fig. 5d, e).

After the borehole installation in October 2012, a saturated zone was identified in the basal section of the tailings. Through piezometer readings, the water table depth ranged from −36.05 m to −34.3 m in June 2014. Thus, the tailing pond possesses a mean saturation thickness of approximately 4 m. Maximum measured oxygen values were identified within the first meter of the tailings (16%) and rapidly decreased until reaching 0.3% at a depth of 5 m. These anoxic environmental conditions were maintained throughout the remainder of the vertical profile, with a complete oxygen absence existing between 6 m and the 35.5 m sensor.

4.3. Tailings and water geochemistry

Table 1 presents the Pb, Zn, Cu, As, Mn, Sr, Rb and Fe contents from the tailing drill core samples, as well as mean values, threshold values and standard intervention values established by authority of the Andalusian Autonomous Community. Note that the mean Pb (2308 mg kg^{-1}), Zn (2141 mg kg^{-1}) and As (180 mg kg^{-1}) levels are all above the established intervention levels.

Table 2 presents the pH, CaCO$_3$, total sulfide, humidity and the sand-silt-clay fraction analyses. The pH values ranged from 6.7 and 8.2 across the borehole, indicating alkaline conditions, which correlate with the CaCO$_3$ concentration. The alkaline pH is attributed to additives, which were introduced during the flotation process to improve lead separation, and carbonate gangue. The total sulfide content varied from less than 0.1 to 0.6 wt.% in the core samples. The maximum values for S^{2-} were found at 13 m depth, and in an intermediate section from 23 to 30 m.

Fig. 5a, b and c illustrate the vertical concentration variations of the studied elements. Fig. 5a shows the vertical Pb, Zn and Mn variations in the deposits. Elevated Pb contents were detected across the entire deposit, with three maximum concentrations associated with an upper section between 1 and 4 m (up to 3195 mg kg^{-1}), an intermediate section between 29 and 31 m (3075 mg kg^{-1}) and a lower section from 35 to 39.3 m. (up to 8065 mg kg^{-1}). High Zn concentrations were found in two zones, from 10 to 15 m (up to 3540 mg kg^{-1}) and from 35 to 39.3 m. (up to 5186 mg kg^{-1}). The vertical Rb, Sr and Cu distributions (Fig. 5b) exhibit minor oscillations around a relatively constant level and without a significant trend. A significant correlation is visible between As, Zn, Fe and S^{2-}, indicating an As association to metal sulfides.

The vertical humidity profile (Fig. 5d) displays an increasing trend with depth. In addition, it exhibits significant oscillations. These oscillations may be related to the micro-scale grain size variability, which can lead to elevated values in clayey areas.

Fig. 5e indicates elevated amounts of sand in the upper 20 m of the pile, which may be related to the source material and mining technology. The grain size distribution is not clearly reflected in the humidity profile or the vertical distributions of the remaining analyzed parameters. However, the large oscillations of the humidity profile may overprint the change between the upper coarse grained area to the lower part below 18 m depth.

Groundwater samples obtained from the piezometer were characterized by conductivity values ranging from 3.14 to 3.33 mS cm^{-1}, temperatures from 17 to 20.7 °C, pH values from 5.9 to 6.9 and oxygen levels from 2 to 6 mg L^{-1}. This circumneutral water exhibited high sulfate (2495 mg L^{-1}), calcium (570 mg L^{-1}), dissolved Fe (20 mg L^{-1}), Mn (16 mg L^{-1}) and Zn (7 mg L^{-1}) contents. Meaningful dissolved As (5–30 μg L^{-1}) and Pb (10–50 μg L^{-1}) concentrations were also detected.

4.4. Statistics

Of the 8 analyzed elements, Pb, Zn, Cu, As, Sr and Fe revealed a wide range of concentrations and high mean values.

The univariate analysis indicated that the means and medians of Pb, As, Zn, Cu and Fe exhibit considerable variations (Table 3). Fig. 6 illustrates the histograms, box and whisker plots and Q–Q graphs of four selected elements: Pb, Cu, Fe and Zn. The histograms are asymmetric, displaying the highest frequencies at the lowest intervals. The boxplots reveal that the medians are displaced in the box in the direction of the first quartile. Four elements possess high values above the upper limit (Pb and Fe levels in the 38.5 and 39.3 m samples, Zn in the 13 and 39.3 m samples and Cu in the 3 and 38.5 m samples). Furthermore, the large standard deviations and variation coefficients, together with the asymmetry and kurtosis values, indicate that the elements have asymmetric distributions with a long tail to the right. The asymmetric distributions are also revealed in the Q–Q graph, where it is evident that the plots are far from the normal theoretical slope. In addition, the Kolmogorov–Smirnov normality test and the Shapiro–Wilk test indicate that these elements do not follow a normal distribution. Note that As, which exhibits high concentration values, does not follow a normal distribution in the deposit. Only Mn and Rb displayed normal distributions in the tailings.

To discriminate between the different groups of metals, an explorative hierarchical cluster analysis was performed on the data set (20 cores samples and 8 elements, without consideration of the 39.4 m phyllite sample). The results (Fig. 7a, cluster of observations) allowed for the identification of two main groups. Group 1/2 (subgroups 1/4 and 2/4) contains the samples collected at 1, 31, 13, 38.5 and 39.3 m. These samples exhibited high contents of a variety of elements. The 1 m sample displayed high contents of Pb, Zn and Fe and a low percentage of CaCO$_3$. The 31 m sample possessed high values of Pb and Fe. Sample 13 also had high Zn, Fe and As contents, a low CaCO$_3$ percentage and a slightly acidic pH. The 38.5 and 39.3 m samples exhibited high Pb, Zn, Fe and As contents, a low CaCO$_3$ percentage and a slightly acidic pH. The 3/4 sub-group, which consisted of the 5, 6, 29.4, 10.2 and 17 m samples, revealed low Pb and Fe contents and high CaCO$_3$ percentages, particularly in the 5 and 6 m samples.

The variable cluster in Fig. 7b identifies two groups, which can be subdivided into three sub-groups. Sub-group 1/3 relates Pb to Fe, which are predominant elements in mineral paragenesis, as compared to Rb. Sub-group 2/3 relates Zn with As, as opposed to Mn. Sub-group 3/3 relates Cu to Sr.

5. Discussion and conclusions

An internal characterization of the La Aquisgrana tailings pond was performed using combined methods of electrical resistivity imaging (ERI) and hydrogeochemical parameters. The generated real resistivity

Table 3
Statistics for drill core data: minimum, maximum, mean, median, standard deviation (SD), variance, variation coefficient (VC), asymmetry (Asym), Kurtosis, Kolmogorovov–Smirnov and Shapiro–Wilk for pH values, CaCO$_3$, sand, lime, and clay contents (wt.%), Sr, Rb, Pb, As, Zn, Cu, Fe and Mn (mg kg^{-1}).

Data	Minimum	Maximum	Mean	Median	SD	Variance	VC (%)	Asym	Kurtosis	Kol-Smir	Shapiro Wilk
pH	6.5	8.3	7.6	7.7	0.5	260	7	−0.75	−0.27	0.15	0.92
CO3Ca	0.7	8.6	3.7	3.1	2.4	55,790,000	64	0.99	0.04	0.22	0.88
Clay	15	40	24	20	8.5	71,637	36	0.81	−0.56	0.25	0.86
Silt	15	50	28	25	11.1	123,065	40	0.78	−0.25	0.22	0.90
Sand	10	70	48	55	18.8	352,173	39	−0.72	−0.63	0.21	0.90
Sr	25	77	32	28	12.5	155,748	39	2.83	8.46	0.34	0.60
Rb	94	141	111	111	11.5	132,929	10	0.69	0.72	0.09	0.96
Pb	485	8065	2221	1534	1862	3,467,978	84	2.10	4.68	0.20	0.76
As	43	544	174	150	132	17,310	76	1.46	2.07	0.17	0.85
Zn	692	5186	2072	1833	896	802,881	43	2.30	7.28	0.27	0.76
Cu	29	531	62	37	108	11,624	175	4.54	20.75	0.46	0.28
Fe	16,353	34,793	21,185	19,746	4460	19,890,631	21	1.85	3.68	0.23	0.81
Mn	138	987	701	722	180	32,579	26	−1.41	3.77	0.18	0.90

model allowed for morphology depiction, as well as identification of vertical and horizontal distribution variations in the tailings.

This information led to the installation of mechanical sounders to cut through the central core of the tailings pond. Physical and chemical data obtained from the drill core samples were used to calibrate the resistivity profile (Figs. 4 and 5). Fig. 5f illustrates the resistivity values extracted from the real resistivity section along the borehole. Sand is the predominant fraction (>60%) in the first 10 m of the profile, exhibiting a low moisture content (approximately 10%). The resistivity values measured in this area are above 50 Ω.m (Fig. 5f). Below this level, there is a slight decrease in the sand content, which is accompanied by an increase in the humidity (30%). This reflects the resistivity decrease, with values between 35–50 Ω.m. The lowest resistivity values measured in the borehole (less than 30 Ω.m) occur between 20–30 m, coinciding with significant increases in both moisture (up to 34%) and silt and clay contents. The highest sulfide content values were also obtained at this level.

This range of low resistivity values is recorded on the surface of the tailings, at the top of the western portion of the profile. Field observations revealed the presence of vegetation, suggesting water infiltration and wet conditions that cause low resistivity values. The remainder of the tailings is covered by a predominantly sandy layer, with measured resistivities above 50 Ω.m.

The lowest portion of the borehole corresponds to the tailings saturated zone, where the groundwater has an average E.C. of 3.3 mS cm^{-1}. This conductivity value is equivalent to a resistivity of approximately 3–5 Ω.m, which coincides with the values measured at the bottom of the western portion of the ERI profile. However, this low resistivity was not identified by the probe in the saturated zone, which is also characterized by higher solid phase metal concentrations. This may be due to limitations associated with the sensitivity and resolution of the geoelectrical method because those measurements approached the lower limit of the model and sharp resistivity contrasts exist between adjacent blocks.

Variable clustering associated Pb with Fe, and both are significant mineral paragenesis elements. In addition, Zn was associated with As and Cu with Sr, as minor elements. The 1/2 cluster reveals that the samples taken at 1, 13, and 38 m exhibit high metallic contents.

Two Pb enriched levels were identified, located in the upper section (0 to 5 m, with a Pb content of up to 3195 mg kg^{-1}) and the lower section (35 to 39.3 m, Pb 8065 mg kg^{-1}). In these sections, high contents of other metals (Cu 531 mg kg^{-1}, Zn 5186 mg kg^{-1} and Fe 34,793 mg kg^{-1}) were also found.

Note that there was an intermediate area in the deposit (from 10 to 15 m), where high concentrations of Zn (3.540 mg kg^{-1}), As (544 mg kg^{-1}) and Fe (2, 5 wt.%) were found, accompanied by a high sulfide content. This association could be related to the presence of sphalerite in the processed materials.

Considering the measured oxygen concentrations, the tailings pond presents a large unoxidized zone of approximately 30 m, with oxygen disappearing at 5 m depth due to high amounts of electron donors. Although low pH values would be expected at the surface due to sulfide mineral weathering, the measured pH is above 7 which is attributed to calcite buffering. However, this is not reflected in lower carbonate content of the oxidized zone indicating a surplus of CaCO$_3$ which has not been entirely consumed by neutralization reactions.

The section from 10 to 15 m, which is Zn, As and Fe enriched, was located in the anoxic zone of the tailings, with pH values buffered due to the presence of carbonates, thus minimizing the risk of sulfide oxidation and metal mobilization. This may be not the case for As because it is highly mobile under neutral and slightly alkaline and under reducing conditions.

The saturated zone registered important seasonal variations in both the water level and dissolved oxygen content. Based on the low precipitation regime in the study area, the thickness of the unsaturated zone (more than 30 m) and the almost complete absence of oxygen above the saturated zone, the vertical infiltration recharge zone is likely scarce. Phyllites exhibit a hydrogeological behavior generally impermeable, and no local groundwater level is associated with these materials. The milonitized and fractured zone, which was identified in the SW sector of the tailings, could be acting as a preferential infiltration zone for subsurface flow. According to the interpretation of the ERI profile, this fractured zone is in contact with the tailings and could contribute to the lateral recharge of the saturated zone.

The saturated zone (the lower 4 m of the tailings pile) coincides with the highest metal concentrations. In addition, the water exhibits elevated dissolved sulfate, iron, manganese and zinc contents, which could be the result of a metal mobilization process. Although generation of acid mine drainage has not occurred due to low oxidative weathering, low CaCO$_3$ concentrations in the saturated part between 34 and 39 m (Table 2) can be attributed to a sulfide oxidation process associated with limited input of oxygen by lateral groundwater inflow commented above (2–6 mg L^{-1} of dissolved oxygen) coupled with calcite buffering. However, this observation is not confirmed by sulfide concentrations indicating that sulfide oxidation has occurred only at a minor degree.

Utilizing various boreholes proved to be a useful technique for achieving our study objectives because borehole sampling allowed for the identification of zones with elevated contamination potential within the heap. Furthermore, the combined use of information provided by the drill core samples and the real resistivity values allow for a geophysical characterization of the entire tailings profile. Contaminated areas of the tailings are characterized by low resistivity values, which were associated with high water contents and elevated solid or dissolved metal concentrations.

Upon identification of the tailings areas with the greatest mobilization risks, concrete solutions can potentially be utilized to mitigate these risks. In this case, remediation actions should focus on the preferential infiltration area, which should reduce the subsurface flow of oxygenated water into the tailings.
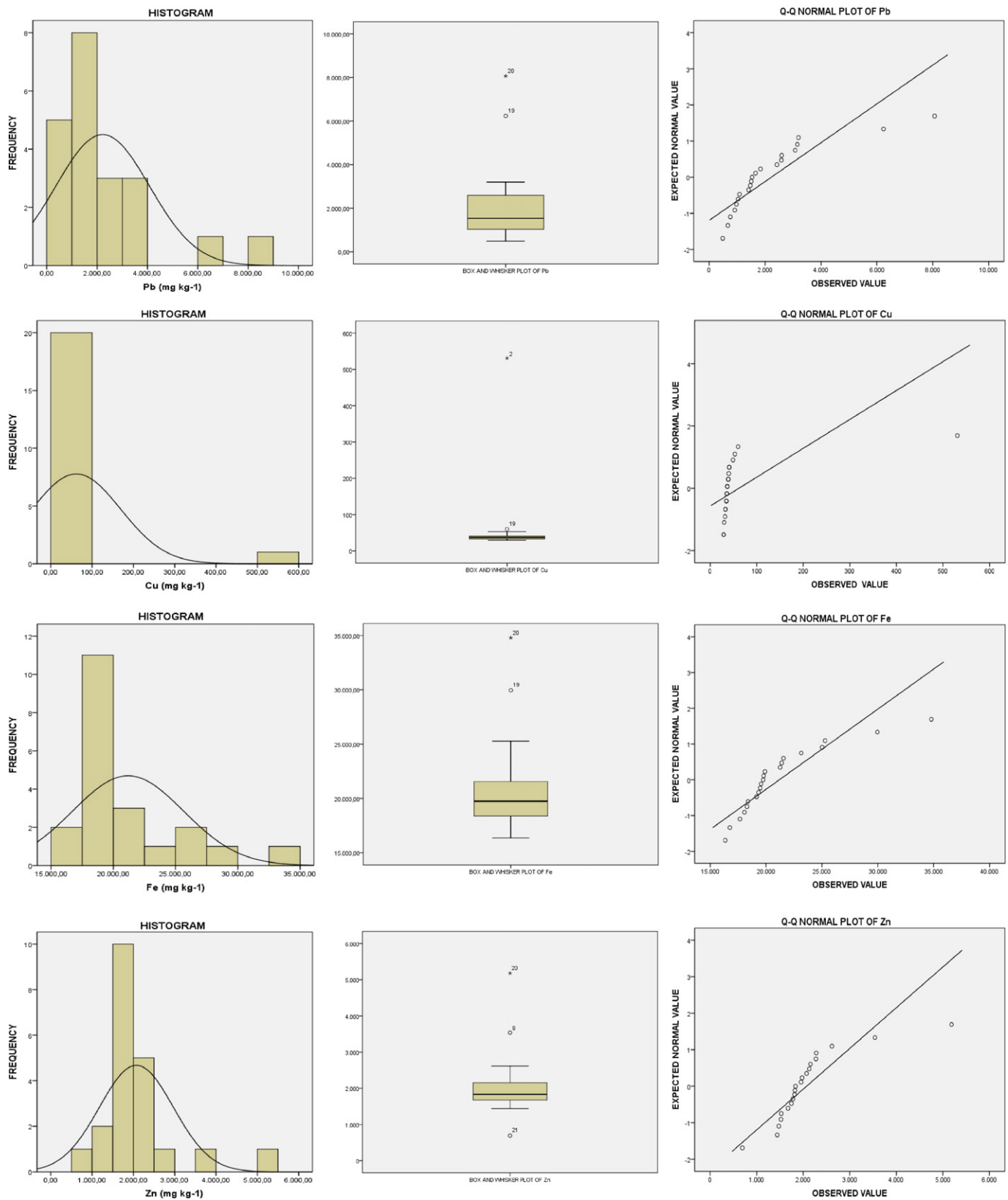
Fig. 6. Histograms, box and whisker plots and Q–Q normal plots of Pb, Cu, Fe and Zn.

The methods described in this work may serve as useful tools that can be applied to various tailings ponds found in ancient mining districts. With the help of these techniques we were able to identify element concentration levels that represent a greater potential risk for contamination.

Acknowledgments
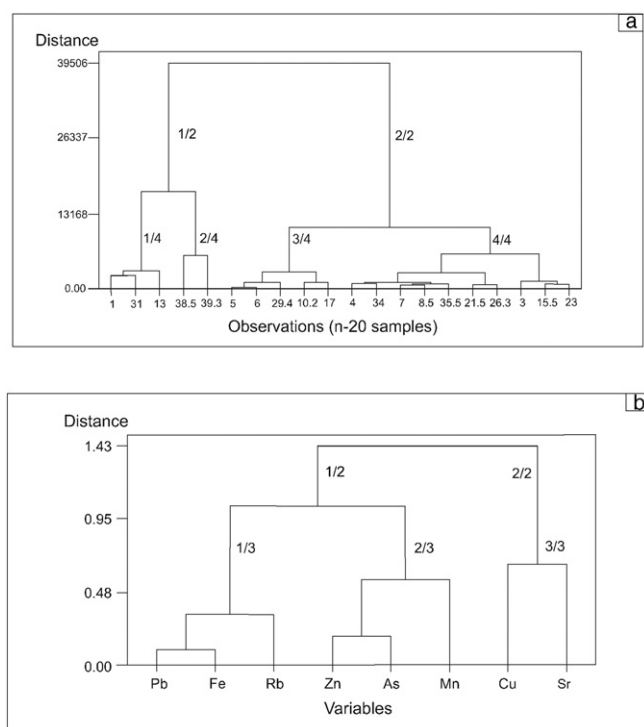
Fig. 7. Cluster analysis of observations (a) and Cluster analysis of variables (b).

References

Bundschuh, J., Litter, M.I., Parvez, F., Román-Ross, G., Nicolli, H.B., Jean, J.S., Liu, C.W., López, D., Armienta, M.A., Guilherme, L., Gomez, A., Cornejo, L., Cumbal, L., Toujaguez, R., 2012. One century of arsenic exposure in Latin America: a review of history and occurrence from 14 countries. Sci. Total Environ. 429, 2–35.

Castelló, R., Orviz, F.,1976. Mapa geológico y memoria explicativa de la hoja n° 884 (La Carolina) del mapa Geológico de España, escala 1:50.000. Instituto Geológico y Minero de España.

Chae Jung, M., 2008. Contamination by Cd, Cu, Pb, and Zn in mine wastes from abandoned metal mines classified as mineralization types in Korea. Environ. Geochem. Health 30, 205–217.

Chopin, E.I.B., Alloway, B.J., 2007. Trace element partitioning and soil particle characterization around mining and smelting areas at Tharsis, Ríotinto and Huelva, SW Spain. Sci. Total Environ. 373, 488–500.

Contreras, F., Dueñas, J., 2010. La minería y la metalurgia en el Alto Guadalquivir: Desde sus orígenes hasta nuestros días. Instituto de Estudios Giennenses, Diputación de Jaén.

Dahlin, T., Zhou, B., 2004. A numerical comparison of 2D resistivity imaging with 10 electrode arrays. Geophys. Prospect. 52, 379–398.

Davis, B.E., 1983. Heavy metal contamination from base metal mining and smelting: implications for man and his environment. In: Thornton, I. (Ed.), Applied Environmental Geochemistry. Academic, London, pp. 425–650.

De la Torre, M.J., Campos, M.J., Hidalgo, M.C., 2010. Estudio mineralógico de las escombreras en el distrito minero de La Carolina. Macla 13, 213–214.

Domínguez, M.T., Alegre, J.M., Madejón, P., Madejón, E., Burgos, P., Cabrera, F., Marañón, T., Murillo, J.M., 2016. River banks and channels as hotspots of soil pollution after large-scale remediation of a river basin. Geoderma 261, 133–140.

Drahor, M.G., 2006. Integrated geophysical studies in the upper part of Sardis archaeological site, Turkey. J. Appl. Geophys. 59, 205–223.

Facchinelli, A., Sacchi, E., Mallen, L., 2001. Multivariate statistical and GIS based approach to identify heavy metal sources in soils. Environ. Pollut. 114, 313–324.

Gallego, J.L.R., Ordóñez, A., Loredo, J., 2002. Investigation of trace element sources from an industrialized area (Avilés, northern Spain) using multivariate statistical methods. Environ. Int. 27, 589–596.

Gómez-Ortiz, D., Martín-Velázquez, S., Martín-Crespo, T., De Ignacio-San José, C., Lillo, J., 2010. Application of electrical resistivity tomography to the environmental characterization of the abandoned massive sulphide mine ponds (Iberian Pyrite Belt, SW Spain). Near Surf. Geophys. 8, 65–74.

Gómez-Ros, J.M., Garcia, G., Peñas, J.M., 2013. Assessment of restoration success of former metal mining areas after 30 years in a highly polluted Mediterranean mining area: Cartagena-La Unión. Ecol. Eng. 57, 393–402.

Griffiths, D.H., Barker, R.D., 1993. Two-dimensional resistivity imaging and modelling in areas of complex geology. J. Appl. Geophys. 29, 211–226.

Guo-Li, Y., Tian-He, S., Peng Han, J.L., 2013. Environmental geochemical mapping and multivariate geostatistical analysis of heavy metals in topsoils of a closed steel smelter: Capital Iron & Steel Factory, Beijing, China. J. Geochem. Explor. 130, 15–21.

Gutiérrez-Guzmán, F., 1999. Las minas de Linares. Apuntes históricos. ColegioOficial de Ingenieros Técnicos de Minas de Linares, Linares.

Gutiérrez-Guzmán, F., 2007. Minería en Sierra Morena, El distrito minero de La Carolina. Ilustre Colegio Oficial de Ingenieros de Minas de Linares.

Huang, W., Campredon, R., Abrao, J.J., Bernat, M., Latouche, C., 1994. Variation of heavy metals in recent sediments from Piratininga Lagoon (Brazil): interpretation of geochemical data with the aid of multivariate analysis. Environ. Geol. 23, 241–247.

Kalogeropulos, N., Karayannis, M.I., Vassililakigrimani, M., Grimanis, A.P., 1994. Application of trace elements determination and multivariate statistics to a pollution study of lake Pamvotis, NW Greece. Fresenius Environ. Bull. 3, 187–192.

Li, X.D., Thornton, I., 1993. Multi-element contamination in soil and plant in the old mining area, O.K. Appl. Geochem. S2, 51–56.

Li, X.D., Thornton, I., 2001. Chemical partitioning of trace and major elements in soils contaminated by mining and smelting activities. Appl. Geochem. 16, 1693–1706.

Lillo, F.J., 1992. Geology and Geochemistry of Linares-La Carolina Pb-ore Field (Southeastern Border of the Hesperian Massif) (Ph.D. thesis, University of Leeds).

Loke, M.H., Barker, R.D., 1996. Rapid least-squares inversion of apparent resistivity pseudosections by a quasi-Newton method. Geophys. Prospect. 44, 131–152.

Loke, M.H., Dahlin, T., 2002. A comparison of the Gauss–Newton and quasi-Newton methods in resistivity imaging inversion. J. Appl. Geophys. 49, 149–162.

Martín-Crespo, T., Gómez-Ortíz, D., Martínez-Pagán, P., De Ignacio-San José, C., Martín-Velázquez, S., Lillo, J., Faz, A., 2012. Geoenvironmental characterization of riverbeds affected by mine tailing in the Mazarrón district (Spain). J. Geochem. Explor. 119-120, 6–16.

Martín-Crespo, T., Gómez-Ortíz, D., Martín-Velázquez, S., Esbrí, J.M., De Ignacio-San José, C., Sánchez-García, M.J., Montoya-Montes, I., Martín-González, F., 2015. Abandoned mine tailings in cultural itineraries: Don Quixote route (Spain). Eng. Geol. 197, 82–93 30 October 2015.

Martín-Crespo, T., Martín-Velázquez, S., Gómez-Ortíz, D., 2010. A geochemical and geophysical characterization of sulfide mine ponds at the Iberian Pyrite Belt (Spain). Water Air Soil Pollut. http://dx.doi.org/10.1007/s11270-010-0595-6.

Martínez, J., 2002. Caracterización geoquímica y ambiental de los suelos en el sector minero de Linares (Ph.D. Thesis, Univ. Politécnica de Madrid).

Martínez, J., Rey, J., Hidalgo, M.C., Benavente, J., 2012. Characterizing abandoned mining dams by geophysical (ERI) and geochemical methods: the Linares-La Carolina district (southern Spain). Water Air Soil Pollut. 223, 2955–2968.

Martinez, J., Rey, J., Hidalgo, M.C., Garrido, J., Rojas, D., 2014. Influence of measurement conditions on resolution of electrical resistivity imaging: the example of abandoned mining dams in the La Carolina district (southern Spain). Int. J. Miner. Process. 133, 67–72.

Martínez-Pagán, P., Faz, A., Acosta, J.A., Carmona, D.M., Martínez-Martínez, S., 2011. A multidisciplinary study for mining landscape reclamation. A study case on two tailing ponds in the region of Murcia (SE Spain). Phys. Chem. Earth 36, 1331–1344.

Martínez-Pagán, P., Faz Cano, A., Aracil, E., Arocena, J.M., 2009. Electrical resistivity imaging revealed the spatial properties of mine tailing ponds in the Sierra Minera of Southeast Spain. J. Environ. Eng. Geophys. 14 (2), 63–76.

Placencia-Gómez, E., Parviainen, A., Hokkanen, T., Loukola-Ruskeeniemi, K., 2010. Integrated geophysical and geochemical study on AMD generation at the Haveri Au–Cu mine tailings, SW Finland. Environ. Earth Sci. 61, 1435–1447.

Reimann, C., Filzmoser, P., 2000. Normal and lognormal data distribution in geochemistry: death of a myth. Consequences for the statistical treatment of geochemical and environmental data. Environ. Geol. 39, 1001–1014.

Reimann, C., Garret, R.G., 2005. Geochemical background—concept and reality. Sci. Total Environ. 350, 12–27.

Ruiz, F., González Regalado, M.L., Borrego, J., Morales, J.A., Pendón, J.G., Muñoz, J.M., 1998. Stratigraphic sequence, elemental concentrations and heavy metal pollution in Holocene sediments from the Tinto-Odiel Estuary, southwestern Spain. Environ. Geol. 34, 270–278.

Sasaki, Y., 1992. Resolution of resistivity tomography inferred from numerical simulation. Geophys. Prospect. 40, 453–464.

Store, H., Storz, W., Jacobs, F., 2000. Electrical resistivity tomography to investigate geological structures of earth's upper crust. Geophys. Prospect. 48, 455–471.

Telford, W.M., Geldart, L.P., Sheriff, R.E., 1990. Applied Geophysics. Cambridge University Press (770 pp.).

Yongming, H., Peixuan, D., Junji, C., Posmentier, E.S., 2006. Multivariate analysis of heavy metal contamination in urban dusts of Xi'an, Central China. Sci. Total Environ. 176-186.

Yuan, G.L., Sun, T.H., Jun Li, P., Lang, X.X., 2014. Source identification and ecological risk assessment of heavy metals in topsoil using environmental geochemical mapping: typical urban renewal area in Beijing, China. J. Geochem. Explor. 136, 40–47.

Zarroca, M., Linares, R., Velásquez-López, P.C., Roqué, C., Rodríguez, R., 2015. Application of electrical resistivity imaging (ERI) to a tailings dam project for artisanal and small-scale gold mining in Zaruma-Portovelo, Ecuador. J. Appl. Geophys. 113, 103–113.

Zhou, B., Dahlin, T., 2003. Properties and effects of measurement errors on 2D resistivity imaging. Near Surf. Geophys. 1, 105–117.